Submitted to:
2001 Particle Accelerator Conference;
June 18-22, 2001; Chicago, IL

BNL-68076

RHIC INSERTION REGION, SHUNT POWER SUPPLY CURRENT ERRORS*

D. Bruno[†], G. Ganetis, R.F. Lambiase, J. Sandberg, Brookhaven National Laboratory
Brookhaven Science Associates, Inc., Upton, Long Island, New York 11973

Abstract

The Relativistic Heavy Ion Collider (RHIC) was commissioned in 1999 and 2000. RHIC requires power supplies to supply currents to highly inductive superconducting magnets. The RHIC Insertion Region contains many shunt power supplies to trim the current of different magnet elements in a large superconducting magnet circuit. Power Supply current error measurements were performed during the commissioning of RHIC. Models of these power supply systems were produced to predict and improve these power supply current errors using the circuit analysis program MicroCap V by Spectrum Software (TM). Results of the power supply current errors are presented from the models and from the measurements performed during the commissioning of RHIC.

1 INTRODUCTION

Simulations of power supply (p.s.) current errors were performed on the RHIC Insertion Region (IR) quadrupole (QUAD) and dipole p.s.'s, as well as the QUAD trim p.s. These simulations were then compared to real p.s. dynamic current errors that were measured. Figure 1 is the current waveform that was used in the simulations. The current ramps up at 25A/s in the main p.s.'s. All of the other IR p.s.'s and QUAD trim p.s.'s track the main p.s. current ramp. There are 5 sections to this ramp. The start of acceleration section is where the greatest p.s. dynamic current error occurs. The start of acceleration section is section 2 of the ramp in Figure 1.

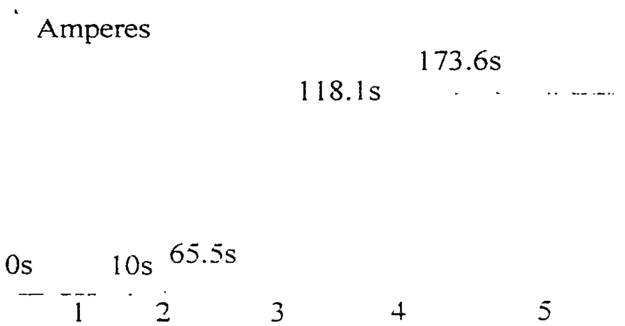

Figure 1: Current Ramp

*Work performed under Contract No. DE-AC02-98CH10886 with the U.S. Department of Energy

[†]bruno@bnl.gov

2 IR QUAD P.S. CURRENT ERRORS

In any sextant of RHIC there can be as many as 7 QUAD p.s.'s nested inside one p.s. The nesting of the IR p.s.'s and the use of superconducting magnets created complex time constants for the current regulator loop which made it very difficult to stabilize the current loops of these p.s.'s. Once the loops were stabilized the p.s. current errors could be measured. The greatest p.s. current error occurs at the start of acceleration region of the ramp. Table 1 contains the measured p.s. current errors at the start of acceleration region of the current ramp for the IR QUAD p.s.'s. This measured error is presented as a percentage of the maximum p.s. current rating. Table 1 also contains the predicted p.s. current errors from the circuit model in MicroCap V. This Model Error is also as a percentage of the maximum p.s. current rating. The p.s. current at the beginning of the ramp and at the end of the ramp is also included in the table for each p.s.

Table 1: IR P.S. Current Errors at Start of Acceleration

Circuits	Start (Amps)	End (Amps)	Measured Error (%)	Model Error (%)
psQ7	41	307	0.09	0.055
psQ456	5.2	35	0.078	0.055
psQ3	-25.5	-168	0.016	0.01
psQ2	10.24	69.4	0.039	0.045
psQ1	2.5	14.6	0.0062	0.0085
psQ3A	-25.5	-168	0.016	0.01
psQ2A	10.24	69.4	0.039	0.045
psQ1A	2.5	14.6	0.0062	0.0085

3 QTRIM P.S. CURRENT ERROR

The QTRIM is a QUAD trim p.s. The QTRIM sets the current difference between the arc horizontal QUADS and the arc vertical QUADS. The main p.s. is hooked up to the horizontal QUADS and vertical QUADS in series. The QTRIM is placed in parallel with the horizontal QUADS and adds current. Again, each QUAD magnet has its own p.s. across it. All of these nested p.s.'s also appear as a load to the QTRIM p.s. which makes it difficult to stabilize the QTRIM p.s. Once the QTRIM p.s. had been stabilized, the p.s. current errors could be measured. Table 2 contains Measured and Modeled QTRIM p.s. current errors at the start of acceleration. These errors were measured and modeled for 3 different types of current regulator cards. Measuring and modeling the p.s. current errors of 3 different current regulator cards helped to reinforce the model. The Type 1 current regulator card was the original card used during the RHIC run in 2001. The Type 1 current regulator card had a 3dB closed loop current Bandwidth (BW) of approximately

Table 2: QTRIM Current Errors at Start of Acceleration

Current Reg. Card	Start (Amps)	End (Amps)	Measured Error (%)	Model Error (%)
Type 1	9	86	0.085	0.087
Type 2	9	86	0.024	0.025
Type 3	9	86	0.014	0.013

2 Hz and a DC gain of 66dB. The Type 2 current regulator card had a 3dB closed loop current BW of approximately 2 Hz and a DC gain of 77dB. The Type 3 current regulator card had a 3dB closed loop current Bandwidth (BW) of approximately 2.4 Hz and a DC gain of 82dB.

4 DHX AND DH0 P.S. CURRENT ERRORS

There are 2 accelerator rings that make up RHIC. They are called the blue ring and the yellow ring. Both rings contain dipole magnets called DH0's. All of the DH0 magnets are connected in series, in each ring, with the main dipole p.s. connected across all of them. There is one main dipole p.s. for the blue ring and one main dipole p.s. for the yellow ring. In addition to the main dipole p.s. being connected across the DH0 magnets there is also a DH0 p.s. connected across each DH0 magnet. These DH0 p.s.'s are nested within the main dipole p.s. The blue ring also contains DHX magnets, the yellow ring does not. These blue DHX magnets are connected in series with the blue DH0 magnets. There are two blue DHX magnets connected in series in between 2 blue DH0 magnets at each sextant of RHIC. In addition there is a blue DHX p.s. connected across each pair of blue DHX magnets. This blue DHX p.s. is nested within the blue DH0 p.s., which is nested within the blue main dipole p.s.

4.1 Blue DHX and DH0 P.S. Current Errors

Five of the six blue ring sextants of RHIC have two DHX magnets and one DHX p.s. nested inside two DH0 magnets and one DH0 p.s. One sextant, at the Ten o'clock region, is different. The DHX and DH0 magnets are not connected in pairs here. There is one DHX magnet with one DHX p.s. nested inside one DH0 magnet and one DH0 p.s. The other DHX magnet is connected within another DHX p.s., which is connected to the other DH0 magnet with another DH0 p.s. across it. P.S. Current errors for these two different configurations are presented in Table 3, Table 4, Table 5 and Table 6.

Table 3: DHX P.S. Current Errors at 2,4,6,8 & 12

Current Reg. Card	Start (Amps)	End (Amps)	Measured Error (%)	Model Error (%)
Type 1	157	982	0.077	0.073
Type 2	157	982	to be done	0.008

In Table 3 the p.s. current errors are presented for the start of acceleration region of the ramp for the blue DHX p.s.'s at the 2, 4, 6, 8 and 12 o'clock insertion regions. The Type 1 current regulator card has been tested but the Type 2 has not been tested yet. Type 1 has a 3dB closed loop current BW of approximately 0.43 Hz and a DC gain of 66dB. Type 2 has a 3dB closed loop current BW of approximately 3.77 Hz and a DC gain of 85dB.

Table 4: DH0 P.S. Current Errors at 2,4,6,8 & 12

Current Reg. Card	Start (Amps)	End (Amps)	Measured Error (%)	Model Error (%)
Type 1	-16	-93	0.08	0.075
Type 2	-16	-93	to be done	0.016
Type 3	-16	-93	to be done	0.008

In Table 4 the p.s. current errors are presented for the start of acceleration region of the ramp for the blue DH0 p.s.'s at the 2, 4, 6, 8 and 12 o'clock insertion regions. The Type 1 current regulator card has been tested but the Type 2 and Type 3 have not been tested yet. Type 1 has a 3dB closed loop current BW of approximately 3 Hz and a DC gain of 63dB. Type 2 has a 3dB closed loop current BW of approximately 5.24 Hz and a DC gain of 77dB. Type 3 has a 3dB closed loop current BW of approximately 17 Hz and a DC gain of 83dB.

Table 5: DHX P.S. Current Errors at 10

Current Reg. Card	Start (Amps)	End (Amps)	Measured Error (%)	Model Error (%)
Type 1	157	982	0.04	0.042
Type 2	157	982	to be done	0.005

In Table 5 the p.s. current errors are presented for the start of acceleration region of the ramp for the blue DHX p.s.'s at the 10 o'clock insertion region. The Type 1 current regulator card has been tested but the Type 2 has not been tested yet. Type 1 has a 3dB closed loop current BW of approximately 0.485 Hz and a DC gain of 66dB. Type 2 has a 3dB closed loop current BW of approximately 1.7 Hz and a DC gain of 85dB.

Table 6: DH0 P.S. Current Errors at 10

Current Reg. Card	Start (Amps)	End (Amps)	Measured Error (%)	Model Error (%)
Type 1	-16	-93	0.034	0.035
Type 2	-16	-93	to be done	0.004

In Table 6 the p.s. current errors are presented for the start of acceleration region of the ramp for the blue DH0 p.s.'s at the 10 o'clock insertion region. The Type 1 current regulator card has been tested but the Type 2 has not been tested yet. Type 1 has a 3dB closed loop current BW of approximately 3 Hz and a DC gain of 63dB. Type

2 has a 3dB closed loop current BW of approximately 16Hz and a DC gain of 83dB.

4.2 Yellow DH0 P.S. Current Errors

Five of the six yellow ring sextants of RHIC have two DH0 magnets connected in series with a DH0 p.s. connected across both of these DH0 magnets. This DH0 p.s. is nested within the main yellow dipole p.s. The other yellow ring sextant at the 10 o'clock insertion region has the two DH0 magnets split up with a separate yellow DH0 p.s. across each yellow DH0 magnet. These yellow DH0 p.s.'s are still nested within the main yellow dipole p.s. In Table 7 the p.s. current errors are presented for the start of acceleration region of the ramp for the yellow DH0 p.s.'s at the 2, 4, 6, 8 and 12 o'clock insertion regions.

Table 7: DH0 P.S. Current Errors at 2,4,6,8 & 12

Current Reg. Card	Start (Amps)	End (Amps)	Measured Error (%)	Model Error (%)
Type 1	-16	-93	0.011	0.013
Type 2	-16	-93	0.002	0.003
Type 3	-16	-93	0.001	0.001
Type 4	-16	-93	to be done	0.0005

The Type 1, Type 2 and Type 3 current regulator cards have been tested but the Type 4 current regulator card has not been tested yet. Type 1 has a 3dB closed loop current BW of approximately 0.5 Hz and a DC gain of 54dB. Type 2 has a 3dB closed loop current BW of approximately 1.3 Hz and a DC gain of 68dB. Type 3 has a 3dB closed loop current BW of approximately 2.2 Hz and a DC gain of 74dB. Type 4 has a 3dB closed loop current BW of approximately 6.7 Hz and a DC gain of 83dB.

Table 8: DH0 P.S. Current Errors at 10

Current Reg. Card	Start (Amps)	End (Amps)	Measured Error (%)	Model Error (%)
Type 1	-16	-93	0.0028	0.0022
Type 2	-16	-93	to be done	0.00027

In Table 8 the p.s. current errors are presented for the start of acceleration region of the ramp for the yellow DH0 p.s.'s at the 10 o'clock insertion region. The Type 1 current regulator card has been tested but the Type 2 has not been tested yet. Type 1 has a 3dB closed loop current BW of approximately 1.36 Hz and a DC gain of 64dB. Type 2 has a 3dB closed loop current BW of approximately 12Hz and a DC gain of 82dB.

5 CONCLUSION

Improvements in the dynamic p.s. current errors have been made on some IR p.s.'s and more improvements will be tested and made during the next time RHIC runs starting in May 2001. Table 9 is a summary of the I.R. p.s. circuits along with a p.s. dynamic current error improvement factor. This improvement factor is defined as the highest current error, which is in the Type 1 current regulator card, divided by the lowest current error, which is in the highest Type current regulator card. For example, in Table 2, the QTRIM Type 1 current regulator card had a dynamic error of 0.087% in the model. The QTRIM Type 3 current regulator card had a dynamic error of 0.013% in the model. The improvement factor would be 0.087 divided by 0.013, which is equal to 6.7 for the QTRIM.

Table 9: I.R. P.S. Current Error Improvement

P.S. Circuit	**Improvement Factor**
QTRIM	6.7
Blue DHX at 2,4,6,8, & 12	9.125
Blue DH0 at 2,4,6,8, & 12	9.375
Blue DHX at 10	8.4
Blue DH0 at 10	8.75
Yellow DH0 at 2,4,6,8, & 12	26
Yellow DH0 at 10	8.15

The I.R. QUAD p.s. current errors were also measured and modeled. These measurements and models along with the other p.s. circuits presented show that this model is very good for predicting and improving dynamic p.s. current errors.

6 REFERENCES

[1] The RHIC Design Manual

[2] D. Bruno et al., "RHIC Insertion Region Shunt Power Supply Simulation", PAC'99, March 1999.

[3] D. Bruno et al., "Overview of the RHIC Insertion Region, Sextupole and Snake Power Supply Systems", PAC'01, June 2001.

[4] S. Tepekian et al., "Tuning Curves", April 1994, RHIC Applications Note, Number 23.